

# Supplementary Information for “Simulating weak localization in superconducting quantum circuit”

Yu Chen<sup>1</sup>, P. Roushan<sup>1</sup>, D. Sank<sup>1</sup>, C. Neill<sup>1</sup>, Erik Lucero<sup>1,\*</sup>, Matteo Mariantoni<sup>1,2,†</sup>, R. Barends<sup>1</sup>, B. Chiaro<sup>1</sup>, J. Kelly<sup>1</sup>, A. Megrant<sup>1,3</sup>, J. Y. Mutus<sup>1</sup>, P. J. J. O’Malley<sup>1</sup>, A. Vainsencher<sup>1</sup>, J. Wenner<sup>1</sup>, T. C. White<sup>1</sup>, Yi Yin<sup>1,‡</sup>, A. N. Cleland<sup>1,2</sup>, and John M. Martinis<sup>1,2,§</sup>

<sup>1</sup>*Department of Physics, University of California,  
Santa Barbara, California 93106-9530, USA*

<sup>2</sup>*California NanoSystems Institute, University of California,  
Santa Barbara, CA 93106-9530, USA and*

<sup>3</sup>*Department of Materials, University of California,  
Santa Barbara, California 93106-9530, USA*

---

\* Present address: HRL Laboratories, LLC, Malibu, CA 90265, USA

† Present address: Institute for Quantum Computing and Department of Physics and Astronomy, University of Waterloo, Waterloo, Ontario, Canada N2L 3G1

‡ Present address: Department of Physics, Zhejiang University, Hangzhou 310027, China

§ martinis@physics.ucsb.edu

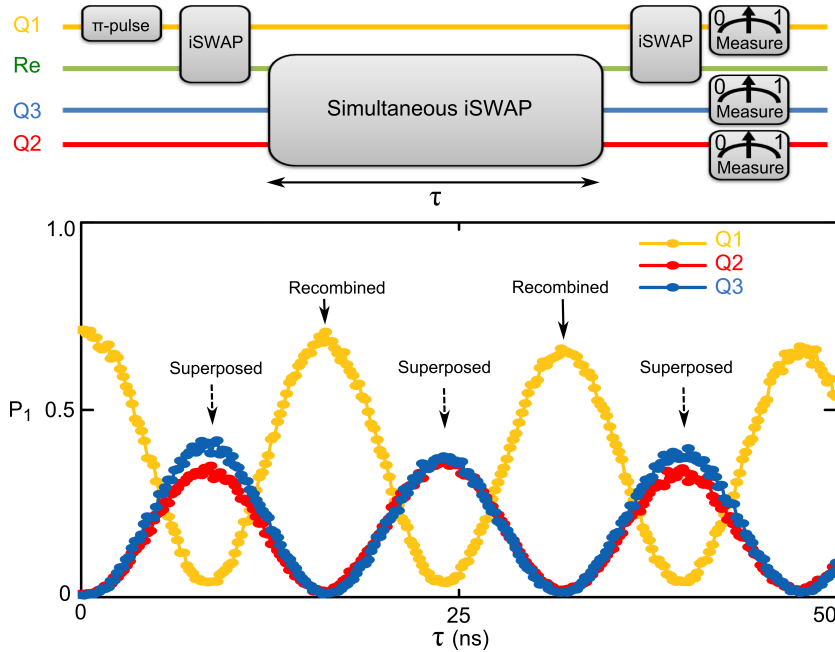


Figure 1. **Upper.** The pulse sequence of distributing the photon between the readout qubit and the two control qubits. **Lower.** The distribution of the photon as a function of the control qubits-resonator interaction time, where we can achieve the superposition and recombination every 8.5 ns.

## I. PHOTON DISTRIBUTION THROUGH THE QUBITS-RESONATOR COLLECTIVE INTERACTION

The simulation of weak localization requires the coherent photon transfer between different quantum elements. In an architecture where all the qubits are symmetrically coupled a center resonator, the quantum circuit provides us a convenient way to coherently transfer a photon between different elements, simply by tuning the qubits in and out of resonance with the resonator.[1] As shown in the pulse sequence in Fig. 1, we realize photon superposition and recombination by distributing the photon between the readout qubit and the control qubits, following the same protocol that has been employed to realize W-type entangled state in superconducting quantum circuits.[2, 3] We first generated a photon in the readout qubit and have it transferred to the coupling resonator. We then immediately detuned the readout qubit back to its idling frequency, while bringing the two control qubits on resonance with the coupling resonator. The two control qubits then remain on resonance with the coupling resonator for a duration  $\tau$ , before we tuned them back to their original frequency and

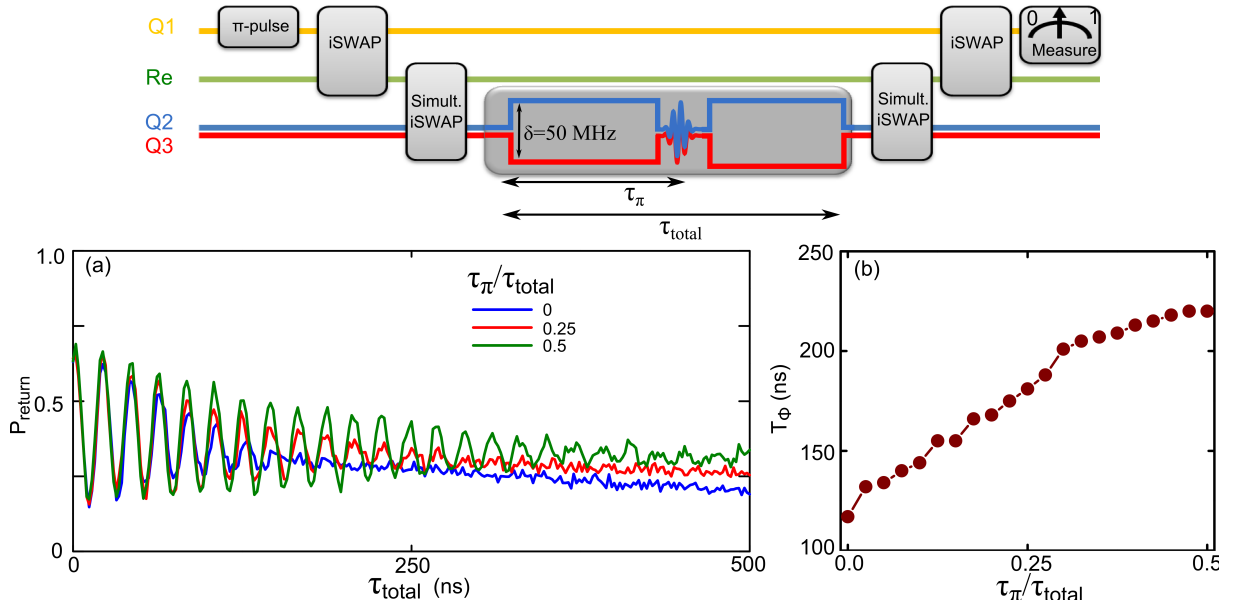


Figure 2. **Upper.** Pulse sequence for the Ramsey-type interference experiment, used to extract the overall coherence time  $T_\varphi$  of the two control qubits. **Lower.** a.  $P_1$  of Q1 as a function of  $\tau_{total}$  obtained from the interference experiment, which we used to demonstrate the tunability of the system phase coherence, as we adjust the ratio of  $\tau_\pi/\tau_{total}$ . b. Extracted system coherence time  $T_\varphi$  as a function of  $\tau_\pi/\tau_{total}$ .

have the remaining photon in the resonator transferred back into the readout qubit. At the end, we perform measurements to all the three qubits, determining the distribution of the photon. The result is demonstrated in Fig. 1, where we plot the probability of measuring the qubits to be in the excited state as a function of the interaction time  $\tau$ . One can see that the photon is initially concentrated in the readout qubit ( $P_1$  maximum for Q1). After an interaction time of 8.5 ns, it splits evenly into the control qubits ( $P_1$  minimum for Q1). By maintaining the interaction for the same duration time, we can reverse the process and have the photon recombine back into the readout qubit.

## II. TUNING THE SYSTEM PHASE COHERENCE TIME

We simulated the temperature effect by tuning the phase coherence time of our superconducting quantum system. One widely used method to improve the system coherence time is the so-called Hahn-echo technique.[4] By inserting a  $\pi$ -pulse into the middle of a pulse se-

quence, one can refocus the phase of the qubit excitation and therefore effectively compensate the system frequency drifting caused by  $1/f$  flux noise. In order to achieve a range of coherence times needed for simulating different temperatures, we apply a modified Hahn-echo sequence, whose effectiveness can be illustrated with a quantum interference experiment. As shown by the pulse sequence in Fig. 2, we first prepare the photon in superposition state of occupying two control qubits, following the method discussed in the previous section. We then apply a constant detuning of 50 MHz between the two control qubits for a total time duration  $\tau_{total}$ , after which the photon gets recombined and subsequently measured by the readout qubit. Within the detuning pulse, we introduce refocusing  $\pi$ -pulses to the two control qubits at a certain time  $\tau_\pi$ , used for effectively tuning the system coherence time. As the results in Fig. 2a shows, when  $\tau_\pi/\tau_{total} = 0$  which corresponds to no refocusing pulse, the interference fringes rapidly decay within the first 150 ns. When  $\tau_\pi/\tau_{total} = 0.5$ , which corresponds to the standard Hahn-echo method, the interference fringes remains visible even over 300 ns, suggesting an improved phase coherence in the system. A tunable coherence time between these two cases can therefore be achieved by adjusting  $\tau_\pi/\tau_{total}$  to have a value between 0 and 0.5, with an example being demonstrated when  $\tau_\pi/\tau_{total} = 0.25$ . From the decay of the amplitude of the interference fringes, we extrapolates the system effective coherence time  $T_{\varphi^{eff}}$ , which basically averaged the dephasing rate of the two control qubits. As shown in Fig. 2b, as we move the location of the refocusing pulse from the beginning to the middle of the detuning sequence, the system effective phase coherence time  $T_{\varphi^{eff}}$  gradually increases from its original value of  $\sim 117$  ns to  $\sim 220$  ns. These values are eventually used to simulate different temperatures in the mesoscopic system.

### III. WEAK ANTI-LOCALIZATION: SPIN EFFECT

The existence of a sizable spin-orbit interaction in the mesoscopic system has profound effects on the weak localization. In meoscopic systems, the spin-orbit coupling induces momentum-dependent spin precession during the scattering events, which shifts the spin phase oppositely for the electron between time-reversed trajectories. The relative phase shift inverts the original time-reversed symmetry into anti-symmetry, which results in the well-known weak anti-localization.[5–8] To simulate the effect of the added phase shift, we

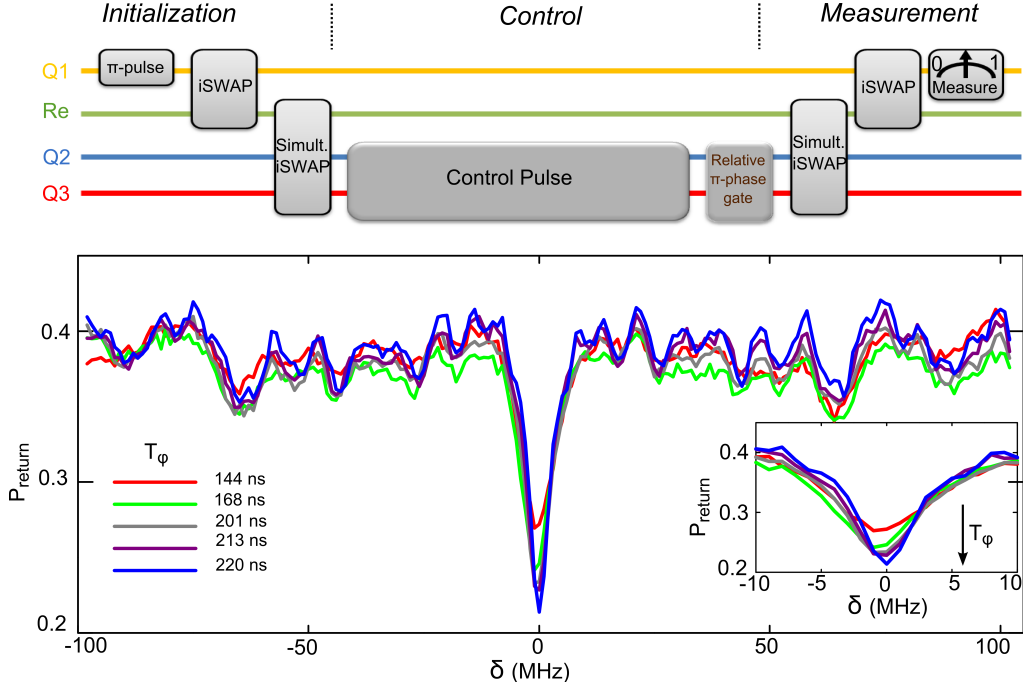


Figure 3. **Upper.** Pulse sequence of simulating weak antilocalization, where we append an additional detuning pulse to accumulate a relative  $\pi$  phase between splitted photon. **Lower.** The measured photon return probability  $P_{\text{return}}$  as a function of the static detuning  $\delta$ , at different coherence time  $T_{\varphi^{\text{eff}}}$ . The  $P_{\text{return}}$  peak at zero detuning resembles the positive magnetoresistance peak associated with weak antilocalization. Inset shows a magnified view of  $P_{\text{return}}$  near  $\delta = 0$ , where we can observe the growth of the  $P_{\text{return}}$  valley, simulating the growth of the magnetoresistance valley when lowering the temperature.

reprogram our pulse sequences by appending an extra detuning pulse to the end of the Control part of the pulse sequence, as shown in the top panel of Fig. 3. The appended detuning pulse was precisely calibrated to induce a relative  $\pi$  phase rotation between the splitted photon, which leads to the reversal of the symmetry between the random detuning pulses. Running the reprogrammed sequence, we remeasure  $P_{\text{return}}$  as a function of the detuning  $\delta$ , with the result demonstrated in Fig. 3. Under the symmetry inversion, the photon now gains a higher probability to return as we turned on the detuning  $\delta$ . The observation of the enhanced photon return probability under the applied detuning  $\delta$  corresponds to the positive magneto-resistance in the mesoscopic system, the experimental signature of the weak anti-localization. We further investigated the temperature effect on the weak anti-localization by including the Hahn-echo refocusing pulse into the sequence. As detailed data

shown in the inset of the figure, the simulated weak anti-localization gradually loses its visibility as we tuned down the quantum coherence of the system. This result is in agreement with well-established experimental observations in mesoscopic systems, where an increased temperature diminishes the amplitude of the positive magneto-resistance. [9]

#### IV. THEORETICAL DISCUSSION ON PHOTON DISTRIBUTION IN TAVIS-CUMMINGS MODEL

Our quantum circuit, with all the qubit symmetrically coupled to the bus resonator, can be described by the Tavis-Cummings model,

$$H = \hbar\omega_r a^\dagger a + \sum_{i=0}^3 \hbar\omega_i \sigma_i^+ \sigma_i^- + \sum_{i=0}^3 \hbar g (a^\dagger \sigma_i^- + a \sigma_i^+), \quad (1)$$

where  $\omega_r, \omega$  are the resonance frequencies of the resonance and qubits, and  $g$  is the coupling strength between the resonator and qubits. This allows for coherent photon transfer directly between qubits and resonator, and indirectly from qubit to qubit via the resonator.

In the case of the photon superposition and recombination, we brought the two control qubits on resonance with the resonator while having the other two qubits far detuned. In this case, we can obtain the matrix for the Hamiltonian in the single photon subspace as

$$H_1 = \begin{bmatrix} \omega & g & g \\ g & \omega & 0 \\ g & 0 & \omega \end{bmatrix}. \quad (2)$$

Diagonalizing the matrix, we can obtain the eigenenergies of the coupled system as  $E_1 = \omega$ ,  $E_2 = \omega + g$  and  $E_3 = \omega - g$ , with three corresponding eigenstates  $|\psi_1\rangle = \frac{1}{\sqrt{2}}(|0eg\rangle - |0ge\rangle)$ ,  $|\psi_2\rangle = \frac{1}{\sqrt{2}}(|1gg\rangle + \frac{1}{2}|0eg\rangle + \frac{1}{2}|0ge\rangle)$  and  $|\psi_3\rangle = \frac{1}{\sqrt{2}}(|1gg\rangle - \frac{1}{2}|0eg\rangle - \frac{1}{2}|0ge\rangle)$ .

For the photon superposition, we initialize the state as  $|\psi(t=0)\rangle = |1gg\rangle$ . The time evolution of the wavefunction can be expressed as

$$|\psi(t)\rangle = \cos\Omega t |1gg\rangle + \frac{i}{2} \sin\Omega t |0eg\rangle + \frac{i}{2} \sin\Omega t |0ge\rangle. \quad (3)$$

We can see that the collective interaction allows the photon to oscillate back and forth between the resonator and two control qubits, at a frequency of  $\Omega = \sqrt{2}g$ . If we set the interaction time to be  $t = (2n + 1)\pi/(2\Omega)$ , with  $n$  being an arbitrary integer number, we can split the photon in the desired superposition state  $|\psi\rangle = \frac{1}{\sqrt{2}}(|0eg\rangle + |0ge\rangle)$ .

For the photon recombination, the initial photon state is  $|\psi(t = 0)\rangle = \frac{1}{\sqrt{2}}(e^{i\phi_1}|0eg\rangle + e^{i\phi_2}|0ge\rangle)$ , where the phases  $\phi_{1,2}$  contains both the random phase and the static phase as described in the main text. Ignoring a global phase and setting  $\phi = \phi_1 - \phi_2$ , we obtain the time evolution of the wavefunction as

$$\begin{aligned} |\psi(t)\rangle &= \frac{i}{2}(e^{i\phi} + 1) \cdot \sin\Omega t |1gg\rangle \\ &+ \frac{1}{2\sqrt{2}}[(1 - e^{i\phi}) + \cos\Omega t \cdot (1 + e^{i\phi})]|0eg\rangle \\ &+ \frac{1}{2\sqrt{2}}[-(1 - e^{i\phi}) + \cos\Omega t(1 + e^{i\phi})]|0ge\rangle. \end{aligned} \quad (4)$$

We set the interaction time to be  $t = (2n + 1)\pi/(2\Omega)$  for a photon recombination. As a consequence, the probability for the photon to be in the resonator, which is eventually measured by Q1, is,

$$P_1 = \frac{1}{2}(1 + \cos\phi). \quad (5)$$

The photon return probability oscillates when we tune the relative phase between two branches of the splitted photon, demonstrating a microwave photon version of the Aharonov–Bohm effect.

In the experiment, the relative phase  $\phi$  was accumulated for a certain detune time  $t$ . During this period of time, the fluctuations in the frequency can lead to the dephasing of the qubits, exhibited as a phase noise  $\Delta\phi$ . Averaged over these phase fluctuations, Eq. (5) gets modified into

$$\begin{aligned} P_1 &= \left\langle \frac{1}{2}(1 + \cos(\phi + \Delta\phi)) \right\rangle \\ &= \frac{1}{2}(1 + \langle \cos\phi \cos(\Delta\phi) \rangle) \\ &= \frac{1}{2}(1 + \cos\phi \langle \cos(\Delta\phi) \rangle), \end{aligned} \quad (6)$$

where we have assumed both qubits to have the same dephasing rate,  $\langle \rangle$  stands for averging over random phase fluctuations and in the last line we have used  $\langle \sin(\Delta\phi) \rangle = 0$ , taking into account of the even distribution of  $\Delta\phi$ .

As thoroughly discussed in Ref. [10], dephasing in this case can lead to the decay of the photon, given as

$$P_1 = \frac{1}{2}(1 + \cos\phi \cdot \exp(-(t/T_{\varphi_1} + (t/T_{\varphi_2})^2)), \quad (7)$$

where the exponential decay originated from the white noise and the Gaussian decay originated from the  $1/f$  noise.

Finally, taking into account for dissipation throughout the sequence, we can obtain the full expression to find the photon back in the resonator as

$$P_1 = \frac{1}{2}(1 + \cos \phi \cdot \exp(-(t/T_{\varphi_1} + (t/T_{\varphi_2})^2)) \exp(-t/T_1). \quad (8)$$

In the experiment, we modulate the effect of the  $1/f$  noise by adjusting the timing of the inserted a  $\pi$ -pulse in the control sequence. In this way, we can effectively modulate  $T_{\varphi_2}$ , which is referred as  $T_{\varphi^{\text{eff}}}$  as in the main text.

- 
- [1] M. Mariani, H. Wang, T. Yamamoto, M. Neeley, R. C. Bialczak, Y. Chen, M. Lenander, E. Lucero, A. D. O'Connell, D. Sank, M. Weides, J. Wenner, Y. Yin, J. Zhao, A. N. Korotkov, A. N. Cleland, and J. M. Martinis, Implementing the quantum von neumann architecture with superconducting circuits, *Science* 334, 6165 (2011).
  - [2] E. Lucero, R. Barends, Y. Chen, J. Kelly, M. Mariani, A. Megrant, P. O'Malley, D. Sank, A. Vainsencher, J. Wenner, T. White, Y. Yin, A. N. Cleland, and J. M. Martinis, Computing prime factors with a josephson phase qubit quantum processor, *Nature Phys.* 8, 719-723 (2012).
  - [3] J. A. Mlynek, A. A. Abdumalikov, J. M. Fink, L. Steen, M. Baur, C. Lang, A. F. van Loo, and A. Wallra, Demonstrating w-type entanglement of dicke states in resonant cavity quantum electrodynamics, *Phys. Rev. A* 86, 053838 (2012).
  - [4] E. L. Hahn, Spin echoes, *Phys. Rev.* 80, 580-594 (1950).
  - [5] J.-B. Yau, E. P. De Poortere, and M. Shayegan, Aharonov-bohm oscillations with spin: Evidence for berry's phase, *Phys. Rev. Lett.* 88, 146801 (2002).
  - [6] G. Bergmann, Weak anti-localization - an experimental proof for the destructive interference of rotated spin 1/2, *Solid State Communications* 42, 815-817 (1982).
  - [7] S. Hikami, A. I. Larkin, and Y. Nagaoka, Spin-orbit interaction and magnetoresistance in the two dimensional random system, *Progress of Theoretical Physics* 63, 707-710 (1980).
  - [8] Y. Meir, Y. Gefen, and O. Entin-Wohlman, Universal effects of spin-orbit scattering in mesoscopic systems, *Phys. Rev. Lett.* 63, 798-800, (1989).

- [9] F. Pierre, A. B. Gougam, A. Anthore, H. Pothier, D. Esteve, and N. O. Birge, Dephasing of electrons in mesoscopic metal wires, *Phys. Rev. B* 68, 085413 (2003).
- [10] J. M. Martinis, S. Nam, J. Aumentado, K. M. Lang, and C. Urbina, Decoherence of a superconducting qubit due to bias noise, *Phys. Rev. B* 67, 094510 (2003).